

# Steady-state properties of a thermodynamically unbalanced Fermi gas

Pedro Ribeiro<sup>1,\*</sup>

<sup>1</sup>*CeFEMA, Instituto Superior Técnico, Universidade de Lisboa Av. Rovisco Pais, 1049-001 Lisboa, Portugal*

The current-carrying steady-state that arises in the middle of a metallic wire connected to macroscopic leads is characterized regarding its response functions, correlations and entanglement entropy. The spectral function and the dynamical structure factor show clear non-equilibrium signatures accessible by state-of-the-art techniques. In contrast with the equilibrium case, the entanglement entropy is extensive with logarithmic corrections at zero-temperature that depend on the wire-leads coupling and, in a non-analytic way, on voltage. This shows that some robust universal quantities found in gapless equilibrium phases do not persist away from equilibrium.

PACS numbers: 73.23.-b, 05.60.Gg, 05.70.Ln

Current-carrying steady-states (CCSS) are characterized by a steady flow of equilibrium-conserved quantities, such as energy, spin or charge. Of direct relevance to transport experiments are steady currents generated by coupling a system to reservoirs at different thermodynamic potentials. The resulting CCSS are thermodynamically unbalanced, i.e. do not fulfill equilibrium fluctuation dissipation relations [1, 2]. CCSS in one or quasi-one-dimensional systems are of relevance in many fields, including charge and spin transport in electronic devices and in cold atom setups.

Due to kinetic constraints, accounting for relaxation in one dimension requires to go beyond 2-body interaction terms and explicitly account for 3- and higher-body collisions [3–5] and thus may be neglected for weakly interacting clean samples. For non-interacting electrons on a wire, ideal reservoirs can be mimicked by injecting particles from plus and minus infinity with a given energy distributions [6–9]. This ideal conditions, alluded to as Landauer reservoirs [10, 11], yield to a local energy distribution function that is the average of those of the leads. A series of studies featuring non-equilibrium Luttinger liquids [12–17] found that interaction-induced dephasing may smear the local energy distribution even in the absence of relaxation. In the presence of a strong enough relaxation the system is expected to equilibrate locally. Treatments based on the Boltzmann equation have been used to obtain the distribution function of the charge carriers in this regime [3–5, 18–20].

Experiments featuring CCSS, designed to access the local energy distribution of charge carries, were performed using tunneling spectroscopy in mesoscopic wires [21–23] and carbon nanotubes [24]. The local energy distribution, measured in the center of the wire, was reported to exhibit a characteristic double step form resulting from contribution of both Fermi functions of the electronic leads. The sharp steps seen at low temperatures are smeared out as temperature increases or in the presence of electron-electron interactions, disorder or electron-phonon coupling.

The study of current-carrying states recently became available for cold atomic setups [25]. Mainly motivated

by these advances, a rather different body of works investigated the time evolution of two initially disconnected semi-infinite wires held at different equilibrium conditions. After the two wires are connected a CCSS forms around the connection point. This central region grows with time, with the remaining parts of the wire acting essentially as reservoirs. At large times a translational invariant CCSS is locally observed [26–35]. Interestingly, some of the properties of the CCSS created in this way, in particular the momentum-resolved electronic distribution, are similar to the CCSS obtained using a Landauer description [26, 29–33, 36]. Furthermore, in both cases, the entanglement entropy of a region in the middle or the wire yields to the same universal result as in equilibrium.

Recently, momentum-resolved spectroscopic measurements became available for non-equilibrium electronic systems [37, 38]. Since to the same local energy spectrum may correspond various momentum distributions, this developments allows a better characterization of the state and may shed some light on discrepancies between existing theoretical predictions and experimental findings. In addition, transport experiments in cold atomic setups [25] allow to access a set of physical quantities that are difficult to study in solid-state devices. These developments urge for a better theoretical understanding of thermodynamically unbalanced CCSS, beyond the local energy distribution function, that is currently still unavailable.

This work addresses the CCSS realized on a finite metallic wire coupled to metallic leads at different temperatures and chemical potentials. The lead-wire couplings are treated explicitly as they induce additional reflections that change the energy distribution of the carries [6, 7]. At equilibrium, the system can be described by an one dimensional electron-gas as we assume no electron-electron interactions or disorder to be present. Our approach describes the low energy sector where the dispersion relation is essentially linear and the reservoirs' chemical potentials and temperatures are much smaller than the wire's bandwidth. We study the one- and two-point functions and analyze the entanglement content in

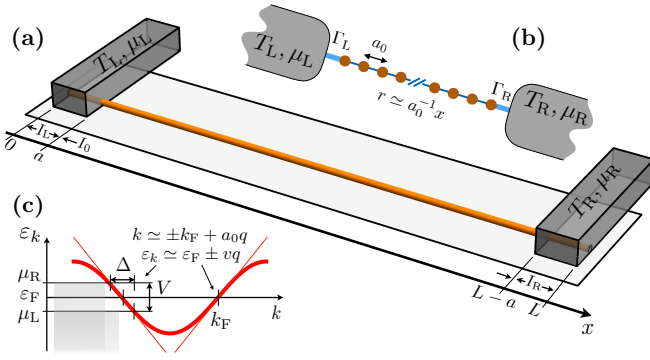


Figure 1. (a) Schematics of the setup. (b) Tight-binding chain coupled to reservoirs. (c) Dispersion relation of the tight-binding chain,  $\varepsilon_k$ , linearized around the Fermi-momentum,  $k_F$ , defined such that  $\varepsilon_{k_F} = (\mu_L + \mu_R)/2$ , with  $V = \mu_L - \mu_R$  and  $\Delta = a_0 V/v$ .

the wire's central region.

*Model and Results.* - Consider the setup of a Fig.1-(a) depicting a 1d fermionic gas on a wire of length  $L$  attached to external leads. In the wire, we assume fermions to have an approximately linear dispersion, with velocity  $v$ , within a window of size  $2\Lambda$  around the Fermi points. The effective Hamiltonian of the isolated metallic wire, valid for energies scales below  $v\Lambda$ , is given by

$$H = -iv \int dx \Psi^\dagger(x) \sigma_z \partial_x \Psi(x), \quad (1)$$

where  $\Psi(x) = \{\psi_L(x), \psi_R(x)\}^T$ , with  $\psi_{l=L,R}(x)$  corresponding to the left and right moving fermions with  $\{\psi_l(x), \psi_l^\dagger(x')\} = \delta_{ll'} \delta(x-x')$ . At position  $x_L = 0$  and  $x_R = L$  the boundary conditions are given by  $\psi_L(x_l) = e^{i\phi_l} \psi_R(x_l)$  with phase shift  $\phi_l$ . To model the leads we assume that the extremities of the wire are connected to fermionic reservoirs within a region of length  $a \ll L$  such as in Fig.1-(a). The reservoirs are assumed to be metallic, with a bandwidth much larger than any characteristic energy scale of the wire. Their chemical potentials  $\mu_{l=L,R}$  and temperatures  $T_{l=L,R} = \beta_{l=L,R}^{-1}$  are taken to be much smaller than the energy cutoff  $v\Lambda$ . The hybridization of the wire with reservoir  $l$  is characterized by the energy scale  $av\gamma_l$ , see [39]. The corresponding timescale  $(av\gamma_l)^{-1}$  gives the characteristic time for a particle in region  $I_{l=L,R}$  to escape the reservoir  $l$ . In the following we set  $\mu_L - \mu_R = V \geq 0$  without loss of generality.

To help validate our analytic treatment we present a set of numerical results for a tight-binding model on a chain of  $N$  sites, with Hamiltonian  $H_{\text{TB}} = -t \sum_{r=1}^N c_r^\dagger c_{r+1} + \text{h.c.}$ , coupled at the two end sites to a wide-band reservoir, as in Fig.2-(b). The reservoir  $l$  introduces an hybridization energy scale  $\Gamma_l = \pi t_l^2 D_l$ , where  $t_l$  is the chain-reservoir hopping and  $D_l$  is the local density of states of the reservoir [39, 40]. The average Fermi mo-

mentum  $k_F$  is defined such that  $\varepsilon_{k_F} = \varepsilon_F = (\mu_L + \mu_R)/2$ , thus for  $q$  smaller than  $\Lambda$ :  $\varepsilon_k \simeq \varepsilon_F \pm vq$  and  $c_r \simeq e^{ik_F r} \psi_L(a_0 r) + e^{-ik_F r} \psi_R(a_0 r)$ , with  $k = \pm k_F + a_0 q$  and  $a_0$  the lattice constant, see Fig.2-(c). Further identification between the continuum and tight-binding models yield to:  $N = La_0^{-1}$ ,  $k_F = \arccos(-\varepsilon_F/2t)$ ,  $v = 2a_0 t \sin k_F$ . and  $\phi_L = 2k_F - \pi$ ,  $\phi_R = -2k_F La_0^{-1} - \pi$ . The relation  $a\gamma_l = \frac{1}{4} \ln \left( -\frac{\Gamma_l^2 t^{-2} - 2t^{-1} \sin k_F \Gamma_l + 1}{\Gamma_l^2 t^{-2} + 2t^{-1} \sin k_F \Gamma_l + 1} \right)$  between the hybridization constants can be derived by matching the imaginary part of the wave vectors [39].

In order to address the properties of the steady-state that forms under the conditions described above we compute the retarded ( $R$ ), advanced ( $A$ ) and Keldysh ( $K$ ) components of the Green's function in the frequency domain. The wide-band nature of the reservoirs considerably simplifies our treatment [40]. In this case, the retarded Green's function is given by  $\mathbf{G}^R(\omega; x, x') = \langle x | (\omega - \mathbf{K})^{-1} | x' \rangle$ , where  $\mathbf{K} = \int dx |x\rangle -iv [\sigma_z \partial_x + \sum_{l=L,R} \gamma_l \Theta[|x-x_l| - a]] \langle x|$  is a non-hermitian operator describing a single particle on a wire with particle sinks in regions  $I_{l=L,R}$ .  $\mathbf{K}$  is diagonalized by left and right eigenvectors  $\langle \tilde{\psi}_n |$  and  $|\psi_n\rangle$ , with eigenvalues  $\lambda_n = vq_n$ . In position space  $\langle \tilde{\psi}_n | x \rangle$  and  $\langle x | \psi_n \rangle$  are plane waves, with a complex valued momentum  $q_n$ , for  $x$  within the regions  $I_{l=L,R}$  defined in Fig.1-(a). The wave amplitudes within each region and the quantization condition  $q_n \equiv -\frac{1}{2L}(\phi_L - \phi_R) + \frac{\pi n}{L} - ia \frac{\gamma_L + \gamma_R}{L}$ , with  $n \in \mathbb{Z}$ , are determined by imposing boundary conditions at  $x = 0, L$ , the continuity of the wave functions at  $x = a, L - a$  and the normalization of the wave-functions  $\langle \tilde{\psi}_n | \psi_{n'} \rangle = \delta_{nn'}$ . The Keldysh component of the Green's function in the steady state, given by  $\mathbf{G}^K = \mathbf{G}^R \Sigma^K \mathbf{G}^A$ , can also be obtained explicitly using essentially the same procedure [39]. For convenience, in the following we analyze the hermitian matrices  $\rho^- = -[\mathbf{G}^R - \mathbf{G}^A]/2\pi i$  and  $\rho^+ = \mathbf{G}^K/(-2\pi i)$  rather than the Green's functions.

We concentrate in the middle region of the wire in the limit  $L \rightarrow \infty$ , in which case the quantities  $\rho_{\text{bulk}}^\pm(\omega; x, x') \equiv \lim_{L \rightarrow \infty} \rho^\pm(\omega; x + L/2, x' + L/2)$  become translational invariant, for finite  $x$  and  $x'$ , and their Fourier components are given by

$$\rho_{\text{bulk}}^\pm(\omega, q) = \text{diag} \{ \rho_L^\pm(\omega, q), \rho_R^\pm(\omega, q) \} \quad (2)$$

with  $\rho_{L/R}^-(\omega, q) = \delta(\omega \mp vq)$  and  $\rho_l^+(\omega, q) = [1 - 2n_l(\omega)] \rho_l^-(\omega, q)$ , for  $|q| < \Lambda$ , and where

$$n_l(\omega) = \frac{b_l}{e^{\beta_l(\omega - \mu_l)} + 1} + \frac{(1 - b_l)}{e^{\beta_l(\omega - \mu_l)} + 1} \quad (3)$$

is the energy distribution function of the  $l$ -movers, with  $\bar{R} = L$ ,  $\bar{L} = R$ ,  $a\gamma_L = \frac{1}{4} \ln \frac{1 - b_R}{1 - b_L}$  and  $a\gamma_R = \frac{1}{4} \ln \frac{b_L}{b_R}$ . Since  $V \geq 0$  we have that  $b_L \geq b_R$ . In [39] we provide

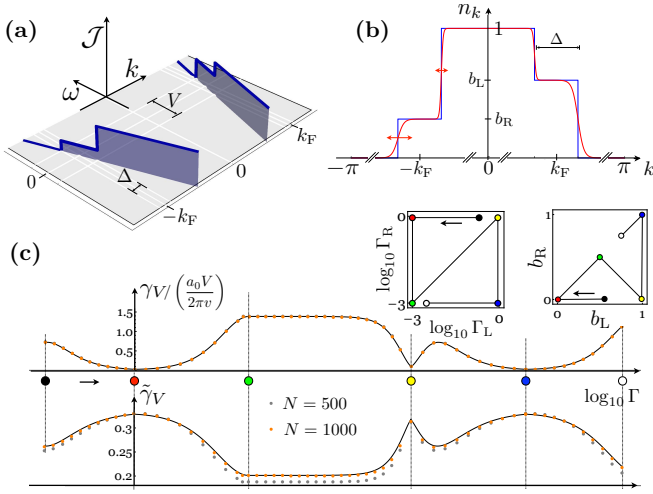


Figure 2. (a)  $\mathcal{J}_k(\omega) = -i\frac{1}{2\pi}G_k^<(\omega)$ , proportional to the transition rate measured by angle-resolved photo emission, for  $T_L, T_R = 0$ . (b) Momentum resolved occupation number  $n_k$  given for  $T_L = T_R = 0$  (blue) and  $T_L > T_R \neq 0$  (red). (c) Extensive coefficient of the entanglement entropy  $\gamma_V$  and the logarithmic correction  $\tilde{\gamma}_V$  computed for set of points  $\{\Gamma_L, \Gamma_R\}$  given in the inset following the color code. The second inset depicts the corresponding  $\{b_L, b_R\}$  values. The numerical values obtained for the tight-binding model with  $\varepsilon_F = .3t$ ,  $V = .2t$ , and  $T_L = T_R = 0$  are compared with the low energy theory predictions (black line).

additional results for  $x$  and  $x'$  near the extremities of the wire, where the state is not translational invariant in the  $L \rightarrow \infty$  limit. Using the correspondence with the continuum model, the tight-binding Green's functions  $G_{rr'}^\alpha(\omega)$ , or equivalently the quantities  $\rho_{rr'}^\pm(\omega)$ , are given by  $\rho_{rr'}^\pm(\omega) = \int_{-\pi}^{\pi} \frac{dk}{2\pi} \rho_k^\pm(\omega) e^{ik(r-r')}$ , for  $r$  and  $r'$  in the middle of the wire, where

$$\rho_k^\pm(\omega) = \rho_L^\pm[\omega, (k - k_F) a_0^{-1}] \Theta(|k - k_F| - \Lambda a_0) + \rho_R^\pm(\omega, k + k_F) \Theta(|k + k_F| - \Lambda a_0). \quad (4)$$

Due to the quadratic nature of the model, these quantities can be used to compute all correlations and response functions restricted to the center of the wire and to low energies. In particular, the single-particle density matrix  $\varrho_{rr'}(t) = \langle c_r^\dagger(t) c_{r'}(t) \rangle$ , that in the steady state is given by  $\varrho_{rr'} = -\pi \int \frac{d\omega}{2\pi} \rho_{r'r}^+(\omega) + \frac{1}{2} \delta_{rr'}$ , can be approximated by

$$\varrho_{rr'} \simeq \varrho_{r-r'} = \int_{-\pi}^{\pi} \frac{dk}{2\pi} e^{-i(r-r')k} n_k, \quad (5)$$

with

$$n_k = n_L \left[ \frac{v}{a_0} (k - k_F) \right] \Theta(|k - k_F| - \Lambda a_0) + n_R \left[ \frac{v}{a_0} (-k_F - k) \right] \Theta(|k + k_F| - \Lambda a_0), \quad (6)$$

the occupation number of momentum  $k$ . This relations can be complemented by  $n_k = 0$  or  $n_k = 1$  away from the range of validity of the low energy theory, i.e.  $|k \pm k_F| > \Lambda a_0$ . Fig. 2-(b) shows  $n_k$  for  $T_L, T_R = 0$  and for finite but distinct  $T_L$  and  $T_R$ . For finite  $V$  there is a double step structure around each Fermi point with width  $\Delta = a_0 V/v$  and height  $b_L$  ( $b_R$ ) for  $k$  near  $k_F$  ( $-k_F$ ). A single step per Fermi point is recovered in three different cases: for reflection-less leads, with  $b_L = 1, b_R = 0$ , reproducing the results obtained using Landauer reservoirs; when one of the leads effectively decouples,  $b_L = 1, b_R = 1$  ( $b_L = 0, b_R = 0$ ), i.e. the wire coupling to the left (right) lead is much larger than that of the right (left), in which case the wire distribution function becomes that of the lead which strongly couples to the system. The steps are smoothen with the temperature associated to the respective of the reservoirs. For  $T_L, T_R \neq 0$ ,  $\varrho_r \propto e^{-|r|/\xi}$  decays exponentially in  $r$ , with a temperature-dependent characteristic length  $\xi$  that diverges as  $T_L$  or  $T_R$  vanish. For  $T_L, T_R = 0$ , one obtains  $\varrho_r = \frac{1}{r} \left\{ \sin\left(\frac{\Delta r}{2}\right) [(b_L - 1) e^{-ir k_F} + b_R e^{ir k_F}] + e^{-\frac{1}{2}i\Delta r} \sin(r k_F) \right\}$ , corresponding to a  $1/r$  decay as in the equilibrium  $T = 0$  case. For reflection-less leads, i.e.  $b_L = 1, b_R = 0$ , the argument of  $\varrho_r$  becomes linear in  $r$ :  $\arg(\varrho_r) = -\frac{1}{2}\Delta r$  as observed in the CCSS formed after a quench in the Refs. [26, 28]. The local distribution function, as measured by tunneling spectroscopy, is  $n_{\text{local}}(\omega) = [n_R(\omega) + n_L(\omega)]/2$ , which for equal contacts (i.e.  $b_L + b_R = 1$ ) becomes independent on  $b_L$ . Tunneling spectroscopy measurements performed with similar contacts can therefore be insensitive to some of the features of  $n_k$ . The particle current  $J = -it \langle c_r^\dagger c_{r+1} - c_{r+1}^\dagger c_r \rangle$ , given in the low energy sector by  $J \simeq \frac{1}{2\pi} (b_L - b_R) V$ , is independent of  $v$  and of the temperature, assuming for consistency  $\Delta \ll 1$ .

In addition to static quantities the CCSS is characterized by its dynamic correlators. Fig. 2-(a) depicts the one point function  $\mathcal{J}_k(\omega) = -i\frac{1}{2\pi}G_k^<(\omega) = \frac{1}{2} [\rho_k^-(\omega) - \rho_k^+(\omega)]$ , that is proportional to the transition rate as measured by angle-resolved photo emission. For  $|\omega| < \Lambda v$  it can be approximated by  $\mathcal{J}_k(\omega) \simeq n_k \{ \delta[\omega - v a_0^{-1}(k - k_F)] + \delta[\omega + v a_0^{-1}(k + k_F)] \}$ , thus the step structure of Fig. 2-(a) is the same of  $n_k$ . Even at zero temperature, there is a non-vanishing probability of finding a particle above  $\varepsilon_F$  for  $V > 0$  and thus  $\mathcal{J}_k(\omega > 0)$  does not vanish.

We now turn to the entanglement properties of the CCSS. The entanglement entropy of a region  $\Sigma$  is defined as  $S_\Sigma = -\text{tr}(\hat{\rho}_\Sigma \ln \hat{\rho}_\Sigma)$  where  $\hat{\rho}_\Sigma = \text{tr}_{\bar{\Sigma}} \hat{\rho}$  is obtained from the total density matrix  $\hat{\rho}$  by tracing out the degrees of freedom belonging to  $\bar{\Sigma}$ , the complement of  $\Sigma$ . In the following we consider a region  $\Sigma_\ell$  of size  $\ell$  in the center of the wire and we denote  $S_\ell = S_{\Sigma_\ell}$ . Since the model is Gaussian  $S_\ell = \text{tr}[s(\varrho_\ell)]$ , with  $s(\nu) = -\nu \ln \nu - (1 - \nu) \ln(1 - \nu)$ , can be computed from

the single particle density matrix  $\varrho_\ell = \sum_{rr' \in \Sigma_\ell} |r\rangle \varrho_{rr'} \langle r'|$  restricted to  $\Sigma_\ell$ .  $S_\ell$  can be calculated, following Ref. [41], using asymptotic results for approximating determinants of Töplitz matrices, valid in the  $\ell \rightarrow \infty$  limit. For  $T_R, T_L \neq 0$  we find, employing Szegő's limit theorem,  $S_\ell = -\ell \sum_l \int_{-\infty}^{\infty} \frac{dk}{2\pi} s[n_k] + \gamma_A$ , where  $\gamma_A$  is an  $\ell$  independent constant. For the case  $T_R, T_L = 0$  we have to appeal to the Fisher-Hartwig conjecture (see [41]) for the case of Fig.2-(b)-(blue line) where  $n_k$  has four discontinuities rather than the two present at equilibrium. Flowing the same steps as in Ref. [41] we obtain, (see [39]),  $S_\ell \simeq \gamma_V \ell + \tilde{\gamma}_V \ln(\ell) + \gamma_A + O(1/\ell)$ , where  $\gamma_V = \frac{a_0 V}{2\pi v} [s(b_L) + s(b_R)]$  is the coefficient of the volume term, and  $\tilde{\gamma}_V = \frac{1}{3} - \tilde{s}(b_L) - \tilde{s}(b_R)$  with

$$\tilde{s}(b) = \frac{1}{24} + \frac{1}{4\pi^2} [(2b-1) [\text{Li}_2(1-b) - \text{Li}_2(b)] + (1-b) \log^2(1-b) + b \log^2(b) + \log(b) \log(1-b)],$$

is the coefficient of the logarithmic correction that is voltage-independent. The mutual information  $S(A, B) = S_A + S_B - S_{A+B}$  between two adjacent segments of length  $\ell/2$ , is given by  $S(A, B) = \tilde{\gamma}_V \ln(\ell) + \gamma_A - 2\tilde{\gamma}_V \ln(2) + O(1/\ell)$ . Here the volume term cancels and we can easily access  $\tilde{\gamma}_V$  numerically. Fig.2-(c) shows  $\gamma_V$  and  $\tilde{\gamma}_V$  as a function of the hybridization along a path in the  $\Gamma_L - \Gamma_R$  plane as well as the corresponding values in the  $b_L - b_R$  plane. With increasing system size the numerical results obtained for the tight-binding model converge to the analytic predictions.  $\gamma_V$  and  $\tilde{\gamma}_V$  vary in the opposite sense - a large volume term corresponds to a small mutual information content. The maximum value  $\tilde{\gamma}_V = 1/3$ , obtained at equilibrium, is attained for  $V > 0$  whenever  $b_L$  and  $b_R$  are such that only two discontinuities arise in  $n_k$ , in which case  $\gamma_V = 0$ . For a generic point on the  $b_L - b_R$  plane with  $\tilde{\gamma}_V \neq 1/3$  the limit  $V \rightarrow 0$  is singular since for  $V = 0$ , and only at that point, one recovers the equilibrium value  $\tilde{\gamma}_V = 1/3$  (numerics shown in [39]). This singularity prohibits the calculation of the entanglement entropy perturbatively in  $V$  and thus this quantity cannot be obtained from linear response arguments.

Finally we analyze the two-point density-density correlations and response functions of the CCSS encoded in the lesser and greater components of the charge susceptibility  $\chi_{rr'}^>(t, t') = -i \langle \hat{n}_r(t) \hat{n}_{r'}(t') \rangle$ ,  $\chi_{rr'}^<(t, t') = -i \langle \hat{n}_{r'}(t) \hat{n}_r(t) \rangle$ . As for the one point function, for  $r, r'$  in the central region of the wire,  $\chi_{rr'}^><$  become approximately translational invariant. In this regime, the Fourier transformed quantities  $\chi_p^\pm(\nu) = -\frac{1}{2\pi i} [\chi_p^>(\nu) \pm \chi_p^<(\nu)]$  are given by

$$\chi_p^\pm(\nu) = [\chi_{LL}^\pm(\nu, a_0^{-1}p) + \chi_{RR}^\pm(\nu, a_0^{-1}p)] + \chi_{LR}^\pm[\nu, a_0^{-1}(p - 2k_F)] + \chi_{RL}^\pm[\nu, a_0^{-1}(p + 2k_F)], \quad (7)$$

where the first two terms correspond to low momentum ( $|p| < a_0\Lambda$ ) and the last two terms to  $2k_F$  contributions

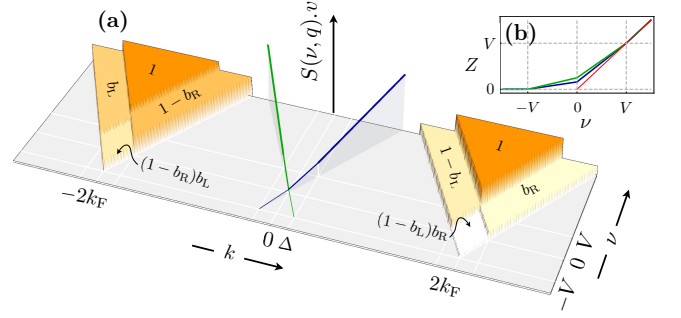


Figure 3. (a) Dynamical structure factor  $S_p(\nu) = i\chi_p^>(\nu)$ , directly accessible by neutron scattering. (b) Weight of the  $\delta$ -function  $Z$  for the positive (blue) and negative (green) velocity branches near  $k = 0$ . The red line depicts the equilibrium, i.e.  $V = 0$ , result.

( $|p - 2k_F| < a_0\Lambda$  and  $|p + 2k_F| < a_0\Lambda$ ) and where

$$\begin{aligned} \chi_{ll}^+(\nu q) &= \frac{1}{2v} \delta(\nu \mp vq) \int \frac{d\omega}{2\pi} [1 - F_l(\omega) F_l(\omega - \nu)], \\ \chi_{ll}^\pm(\nu q) &= \frac{1}{4\pi v} \left[ 1 - F_l\left(\frac{\pm vq + \nu}{2}\right) F_l\left(\frac{\pm vq - \nu}{2}\right) \right], \\ \chi_{ll}^-(\nu q) &= \frac{1}{2v} \delta(\nu \mp vq) \int \frac{d\omega}{2\pi} [F_l(\omega) - F_l(\omega - \nu)], \\ \chi_{ll}^-(\nu q) &= \frac{1}{4\pi v} \left[ F_l\left(\frac{\pm vq + \nu}{2}\right) - F_l\left(\frac{\pm vq - \nu}{2}\right) \right], \end{aligned}$$

where the upper (lower) signs are for  $l = R$  ( $l = L$ ) and  $F_l(\omega) = 1 - 2n_l(\omega)$ . The dynamical structure factor  $S_p(\nu) = i\chi_p^>(\nu)$ , that can be directly accessed by neutron scattering is shown in Fig. 3 for  $T_L = T_R = 0$ . As in equilibrium, the contribution at low momentum is coherent, but the  $\delta$ -function weight  $Z$  acquires a nontrivial dependence on frequency as seen in the inset. Contributions near  $\pm k_F$ , form the particle-hole excitation continuum, also develop a step like structure dependent on  $b_L$  and  $b_R$  that gets smeared out at finite temperatures. In the reflection-less case  $b_L = 1, b_R = 0$  the particle-hole continuum is simply shift up (down) in energy for positive (negative) momentum.

*Conclusion.* - The properties of a CCSS in a thermodynamically unbalanced one-dimensional system are found to crucially depend on the coupling to the leads thought the double-step form of the momentum occupation number near each Fermi point. This feature imprints a clear signature to the one- and two-point functions that are accessible by state-of-the-art angle-resolved photo emission and neutron scattering and can be used to characterize the non-equilibrium state. For a generic CCSS, the entanglement entropy is found to be extensive and proportional to the applied voltage. At zero temperature, the logarithmic pre-factor of the mutual information of two adjacent segments shows that their mutual entanglement is never larger than at equilibrium, being singular at  $V = 0$  and voltage-independent for  $|V| > 0$ . There-



fore, the equilibrium result, that can be obtain by conformal field theory arguments for gapless one-dimensional phases with unit central charge, does not hold away from equilibrium. This suggest that the physics away from equilibrium may be ruled by low energy fixed point theories fundamentally different from the equilibrium ones.

We gratefully acknowledge discussions with D. Esteve, M. Haque, S. Kirchner, A. Lazarides, A. Rubtsov, P. Sacramento and V. R. Vieira. PR acknowledges support by FCT through the Investigador FCT contract IF/00347/2014.

---

\* [ribeiro.pedro@gmail.com](mailto:ribeiro.pedro@gmail.com)

- [1] P. Ribeiro, Q. Si, and S. Kirchner, *EPL (Europhysics Letters)* **102**, 50001 (2013).
- [2] P. Ribeiro, F. Zamani, and S. Kirchner, *Phys. Rev. Lett.* **115**, 220602 (2015).
- [3] A. Levchenko, T. Micklitz, Z. Ristivojevic, and K. A. Matveev, *Phys. Rev. B* **84**, 115447 (2011).
- [4] T. Micklitz and A. Levchenko, *Phys. Rev. Lett.* **106**, 196402 (2011).
- [5] T. Micklitz, A. Levchenko, and A. Rosch, *Phys. Rev. Lett.* **109**, 036405 (2012).
- [6] S. Datta, *Electronic Transport in Mesoscopic Systems* (Cambridge University Press, 1995) Cambridge Books Online.
- [7] J. Imry, *Introduction to Mesoscopic Physics*, Mesoscopic Physics and Nanotechnology (Oxford University Press, 1997).
- [8] M. Di Ventra, *Electrical Transport in Nanoscale Systems* (Cambridge University Press, 2008).
- [9] A. Kamenev, *Field Theory of Non-Equilibrium Systems* (Cambridge University Press, 2011).
- [10] R. Landauer, *IBM Journal of Research and Development* **1**, 223 (1957).
- [11] M. Büttiker, *Phys. Rev. Lett.* **57**, 1761 (1986).
- [12] D. B. Gutman, Y. Gefen, and A. D. Mirlin, *Phys. Rev. Lett.* **101**, 126802 (2008).
- [13] D. B. Gutman, Y. Gefen, and A. D. Mirlin, *Phys. Rev. B* **80**, 045106 (2009).
- [14] S. Ngo Dinh, D. A. Bagrets, and A. D. Mirlin, *Phys. Rev. B* **81**, 081306 (2010).
- [15] S. Takei, M. Milletari, and B. Rosenow, *Phys. Rev. B* **82**, 041306 (2010).
- [16] D. B. Gutman, Y. Gefen, and A. D. Mirlin, *Journal of Physics A: Mathematical and Theoretical* **44**, 165003 (2011).
- [17] V. Popkov, M. Salerno, and G. M. Schütz, *Phys. Rev. E* **85**, 031137 (2012).
- [18] A. M. Lunde, K. Flensberg, and L. I. Glazman, *Phys. Rev. B* **75**, 245418 (2007).
- [19] J. Rech, T. Micklitz, and K. A. Matveev, *Phys. Rev. Lett.* **102**, 116402 (2009).
- [20] A. M. Lunde, A. D. Martino, A. Schulz, R. Egger, and K. Flensberg, *New Journal of Physics* **11**, 023031 (2009).
- [21] H. Pothier, S. Guéron, N. O. Birge, D. Esteve, and M. H. Devoret, *Phys. Rev. Lett.* **79**, 3490.
- [22] H. Pothier, S. Guéron, N. O. Birge, D. Esteve, and M. H. Devoret, *Zeitschrift für Physik B Condensed Matter* **103**, 313 (1997).
- [23] A. Anthore, F. Pierre, H. Pothier, and D. Esteve, *Phys. Rev. Lett.* **90**, 076806 (2003).
- [24] Y.-F. Chen, T. Dirks, G. Al-Zoubi, N. O. Birge, and N. Mason, *Phys. Rev. Lett.* **102**, 036804 (2009).
- [25] J.-P. Brantut, J. Meineke, D. Stadler, S. Krinner, and T. Esslinger, *Science* **337**, 1069 (2012).
- [26] J. Lancaster and A. Mitra, *Phys. Rev. E* **81**, 061134 (2010).
- [27] J. Lancaster, T. Giamarchi, and A. Mitra, *Phys. Rev. B* **84**, 075143 (2011).
- [28] T. Sabetta and G. Misguich, *Phys. Rev. B* **88**, 245114 (2013).
- [29] D. Bernard and B. Doyon, *Journal of Physics A: Mathematical and Theoretical* **45**, 362001 (2012).
- [30] D. Bernard and B. Doyon, *Annales Henri Poincaré* **16**, 113 (2014).
- [31] P. Calabrese, C. Hagendorf, and P. L. Doussal, *Journal of Statistical Mechanics: Theory and Experiment* **2008**, P07013 (2008).
- [32] V. Eisler and Z. Rácz, *Phys. Rev. Lett.* **110**, 060602 (2013).
- [33] V. Alba and F. Heidrich-Meisner, *Phys. Rev. B* **90**, 075144 (2014).
- [34] Y. Ogata, *Phys. Rev. E* **66**, 016135 (2002).
- [35] D. Karevski and T. Platini, *Phys. Rev. Lett.* **102**, 207207 (2009).
- [36] J. Viti, J.-M. Stéphan, J. Dubail, and M. Haque, ArXiv e-prints (2015), [arXiv:1507.08132 \[cond-mat.stat-mech\]](https://arxiv.org/abs/1507.08132).
- [37] I. Gierz, J. C. Petersen, M. Mitrano, C. Cacho, I. C. E. Turcu, E. Springate, A. Stöhr, A. Köhler, U. Starke, and A. Cavalleri, *Nat Mater* **12**, 1119 (2013).
- [38] F. Cilento, S. Dal Conte, G. Coslovich, S. Peli, N. Nembrini, S. Mor, F. Banfi, G. Ferrini, H. Eisaki, M. K. Chan, C. J. Dorow, M. J. Veit, M. Greven, D. van der Marel, R. Comin, A. Damascelli, L. Rettig, U. Bovensiepen, M. Capone, C. Giannetti, and F. Parmigiani, *Nat Commun* **5** (2014).
- [39] “Supplemental material.”
- [40] P. Ribeiro and V. R. Vieira, *Phys. Rev. B* **92**, 100302 (2015).
- [41] A. R. Its and V. E. Korepin, *Journal of Statistical Physics* **137**, 1014 (2009).

– Supplemental Material –

# Steady-state properties of a thermodynamically unbalanced Fermi gas

Pedro Ribeiro<sup>1</sup>

<sup>1</sup>*CeFEMA, Instituto Superior Técnico, Universidade de Lisboa Av. Rovisco Pais, 1049-001 Lisboa, Portugal*

In the following supplemental material we provide additional details of the analytical and numerical analysis performed in the main text. In particular we provide: a derivation of the relations between quantities of the tight-binding and of the continuum model; the derivation of the retarded, advanced and Keldysh Green's functions, and, of the infinite volume limit; we also provide additional the numerical results, for finite and infinite volume, of the one-point function; we present the detailed derivation of the entanglement entropy and give some additional numerical results; and we derive of the two-point function.

## 1 – IDENTIFICATIONS WITH THE TIGHT-BINDING MODEL I - GREEN'S FUNCTIONS

### 1.1 – Green's functions

Using that, in the low energy sector,  $c_r \simeq e^{ik_{\text{F}}r} \psi_{\text{L}}(a_0 r) + e^{-ik_{\text{F}}r} \psi_{\text{R}}(a_0 r)$  the Green's function of the tight-binding model on the Keldysh contour can be approximated by

$$G_{rr'}(z, z') \equiv -i \langle T_{\gamma} c_r(z) \cdot c_{r'}^{\dagger}(z') \rangle \simeq \begin{pmatrix} e^{ik_{\text{F}}r} & e^{-ik_{\text{F}}r} \end{pmatrix} \cdot \mathbf{G}(z r a_0^{-1}, z' r' a_0^{-1}) \cdot \begin{pmatrix} e^{-ik_{\text{F}}r'} \\ e^{ik_{\text{F}}r'} \end{pmatrix}, \quad (\text{SM-1})$$

where

$$\mathbf{G}(zx, z'x') \equiv -i \langle T_{\gamma} \Psi(zx) \cdot \Psi^{\dagger}(z'x') \rangle, \quad (\text{SM-2})$$

is the continuum Green's function and  $T_{\gamma}$  is the time ordered operator for two times  $z$  and  $z'$  on the Keldysh contour  $\gamma$ . We use the standard definitions of larger and lesser Green's functions,  $\mathbf{G}^{>(<)}(tx, t'x') \equiv \mathbf{G}(tx, t'x')$  for  $z = t$  ( $z' = t'$ ) coming after  $z' = t'$  ( $z = t$ ) along  $\gamma$ , and

$$\mathbf{G}^R(tx, t'x') \equiv \Theta(t - t') [\mathbf{G}^>(tx, t'x') - \mathbf{G}^<(tx, t'x')], \quad (\text{SM-3})$$

$$\mathbf{G}^A(tx, t'x') \equiv -\Theta(t' - t) [\mathbf{G}^>(tx, t'x') - \mathbf{G}^<(tx, t'x')], \quad (\text{SM-4})$$

$$\mathbf{G}^K(tx, t'x') \equiv \mathbf{G}^>(tx, t'x') + \mathbf{G}^<(tx, t'x'). \quad (\text{SM-5})$$

Below we will use the notation  $\mathbf{G}^a(tx, t'x') = \langle x | \mathbf{G}^a(t, t') | x' \rangle$ , for  $a = R, A, K$ , and in the steady-state we define  $\mathbf{G}^a(\omega) = \int \frac{d\omega'}{2\pi} e^{i\omega(t-t')} \mathbf{G}^a(t, t')$ . For convenience we work with the quantities

$$\rho^{-}(\omega) = - [\mathbf{G}^R(\omega) - \mathbf{G}^A(\omega)] / (2\pi i), \quad (\text{SM-6})$$

$$\rho^{+}(\omega) = -\mathbf{G}^K(\omega) / (2\pi i), \quad (\text{SM-7})$$

rather than the Green's functions themselves. These are proportional to the spectral function and to the imaginary part of the Keldysh Green's function, respectively, and encode the same physical information. Note that defined in this way both  $\rho^{\pm}$  are hermitian matrices  $(\rho^{\pm})^{\dagger} = \rho^{\pm}$ . As in Eq.(SM-1), we also have the relation

$$\rho_{rr'}^{\pm}(\omega) \simeq \begin{pmatrix} e^{ik_{\text{F}}r} & e^{-ik_{\text{F}}r} \end{pmatrix} \cdot \rho^{\pm}(\omega; r a_0^{-1}, r' a_0^{-1}) \cdot \begin{pmatrix} e^{-ik_{\text{F}}r'} \\ e^{ik_{\text{F}}r'} \end{pmatrix}, \quad (\text{SM-8})$$

between continuum and tight-binding quantities.

## 2 – SINGLE PARTICLE CORRELATION FUNCTIONS

### 2.1 – Self-energies

The reservoirs are assumed to be metallic with a bandwidth much larger than any characteristic energy scale of the wire. In this limit the retarded ( $R$ ) and advanced ( $A$ ) components of the systems's self-energy due to the reservoir  $l$  are given by (see [40])

$$\Sigma_l^{R/A}(\omega; xx') = \mp i\delta(x - x') v \gamma_l \Theta[|x - x_l| - a]$$

where  $\Theta(x)$  is the Heaviside theta-function,  $\gamma_l$  is a constant that characterizes the hybridization of the wire with reservoir  $l$ . Since the reservoirs are taken to be at thermal equilibrium the Keldysh ( $K$ ) component is given by

$$\Sigma_l^K(\omega; xx') = \tanh\left[\frac{\beta_l}{2}(\omega - \mu_l)\right] [\Sigma_l^R(\omega; xx') - \Sigma_l^A(\omega; xx')].$$

The total self-energy is the sum of the contributions of both reservoirs  $\Sigma^{R/A/K} = \sum_l \Sigma_l^{R/A/K}$ .

### 2.2 – Diagonalization of the $K$ operator

Following Ref.[40] we can write the retarded steady-state Green's function in the wide band approximation as  $G^R(\omega) = (\omega - K)^{-1}$ , where the operator  $K$  is given by

$$\mathbf{K} = \int dx |x\rangle \left[ -iv\sigma_z \partial_x - iv\sigma_0 \sum_l \gamma_l \Theta(|x - x_l| - a) \right] \langle x|, \quad (\text{SM-1})$$

with boundary conditions imposed by  $\mathbf{S}_l \langle x_l | \psi \rangle = \langle x_l | \psi \rangle$  with

$$\mathbf{S}_l = \begin{pmatrix} 0 & e^{i\phi_l} \\ e^{-i\phi_l} & 0 \end{pmatrix}. \quad (\text{SM-2})$$

For  $|\psi\rangle$  and  $\langle \tilde{\psi}|$ , respectively right and left eigenvectors  $\mathbf{K}$ , the relations  $\langle x | \mathbf{K} | \psi \rangle = \lambda \langle x | \psi \rangle$  and  $\langle \tilde{\psi} | \mathbf{K} | x \rangle = \lambda \langle \tilde{\psi} | x \rangle$  imply that, for  $x$  within the regions  $I_{l=R,0,L}$ , defined in Fig.1-(a) in the main text,

$$\langle x \in I_l | \psi \rangle = \begin{pmatrix} A_l e^{i(q+i\gamma_l)x} \\ B_l e^{-i(q+i\gamma_l)x} \end{pmatrix}; \quad (\text{SM-3})$$

$$\langle \tilde{\psi} | x \in I_l \rangle = ( \tilde{A}_l e^{-i(q+i\gamma_l)x} \quad \tilde{B}_l e^{i(q+i\gamma_l)x} ); \quad (\text{SM-4})$$

with  $\lambda = vq$  and  $\gamma_0 = 0$ . From the boundary conditions at  $x_L = 0$  and  $x_R = L$  we have

$$B_L = e^{-i\phi_L} A_L; \quad (\text{SM-5})$$

$$B_R = e^{-i\phi_R} e^{2i(q+i\gamma_R)L} A_R; \quad (\text{SM-6})$$

$$\tilde{B}_L = e^{i\phi_L} \tilde{A}_L; \quad (\text{SM-7})$$

$$\tilde{B}_R = e^{i\phi_R} e^{-2i(q+i\gamma_R)L} \tilde{A}_R. \quad (\text{SM-8})$$

In the same way, by ensuring the continuity of the wave function at  $x = a$  and  $x = L - a$  we obtain

$$\begin{pmatrix} A_L e^{i(q+i\gamma_L)a} \\ B_L e^{-i(q+i\gamma_L)a} \end{pmatrix} = \begin{pmatrix} A_0 e^{iqa} \\ B_0 e^{-iqa} \end{pmatrix}; \quad (\text{SM-9})$$

$$\begin{pmatrix} A_0 e^{iq(L-a)} \\ B_0 e^{-iq(L-a)} \end{pmatrix} = \begin{pmatrix} A_R e^{i(q+i\gamma_R)(L-a)} \\ B_R e^{-i(q+i\gamma_R)(L-a)} \end{pmatrix}; \quad (\text{SM-10})$$

$$(\tilde{A}_L e^{-i(q+i\gamma_L)a} \quad \tilde{B}_L e^{i(q+i\gamma_L)a}) = (\tilde{A}_0 e^{-iqa} \quad \tilde{B}_0 e^{iqa}); \quad (\text{SM-11})$$

$$(\tilde{A}_0 e^{-iq(L-a)} \quad \tilde{B}_0 e^{iq(L-a)}) = (\tilde{A}_R e^{-i(q+i\gamma_R)(L-a)} \quad \tilde{B}_R e^{i(q+i\gamma_R)(L-a)}); \quad (\text{SM-12})$$

Combining these results yields to

$$A_0 = B_0 e^{i\phi_L} e^{-2\gamma_L a}; \quad (\text{SM-13})$$

$$A_0 = B_0 e^{-2iqL} e^{i\phi_R} e^{2\gamma_R a}; \quad (\text{SM-14})$$

$$\tilde{A}_0 = \tilde{B}_0 e^{-i\phi_L} e^{2\gamma_L a}; \quad (\text{SM-15})$$

$$\tilde{A}_0 = \tilde{B}_0 e^{-i\phi_R} e^{2iqL} e^{-2\gamma_R a}. \quad (\text{SM-16})$$

Solving for the amplitudes of the central region one obtains

$$\begin{pmatrix} 1 & e^{i\phi_L} e^{-2\gamma_L a} \\ e^{2iqL} e^{-i\phi_R} e^{-2\gamma_R a} & 1 \end{pmatrix} \begin{pmatrix} A_0 \\ B_0 \end{pmatrix} = 0 \quad (\text{SM-17})$$

corresponding to the quantization condition

$$1 - e^{i(\phi_L - \phi_R)} e^{-2(\gamma_L a + \gamma_R a)} e^{2iqL} = 0, \quad (\text{SM-18})$$

i.e.

$$q_n = -\frac{1}{2L} (\phi_L - \phi_R) + \frac{\pi n}{L} - ia \frac{\gamma_L + \gamma_R}{L}, \quad (\text{SM-19})$$

with  $n \in \mathbb{Z}$ . Finally the normalization condition

$$\langle \tilde{\psi}_n | \psi_n \rangle = (\tilde{A}_0 A_0 + \tilde{B}_0 B_0) L = 2\tilde{B}_0 B_0 L = 1 \quad (\text{SM-20})$$

yields to

$$\langle x \in I_L | \psi \rangle = \frac{1}{\sqrt{2L}} \begin{pmatrix} e^{(a-x)\gamma_L + iqx} \\ e^{(a+x)\gamma_L - i(\phi_L + qx)} \end{pmatrix} \quad (\text{SM-21})$$

$$\langle x \in I_0 | \psi \rangle = \frac{1}{\sqrt{2L}} \begin{pmatrix} e^{iqx} \\ e^{-i(2ia\gamma_L + \phi_L + qx)} \end{pmatrix} \quad (\text{SM-22})$$

$$\langle x \in I_R | \psi \rangle = \frac{1}{\sqrt{2L}} \begin{pmatrix} e^{-\gamma_R(a-L+x) + iqx} \\ e^{-\gamma_R(a+L-x) + i(2Lq - qx - \phi_R)} \end{pmatrix} \quad (\text{SM-23})$$

and

$$\langle \tilde{\psi} | x \in I_L \rangle = \frac{1}{\sqrt{2L}} ( e^{(x-a)\gamma_L - iqx} \ e^{i(i(a+x)\gamma_L + \phi_L + qx)} ) \quad (\text{SM-24})$$

$$\langle \tilde{\psi} | x \in I_0 \rangle = \frac{1}{\sqrt{2L}} ( e^{-iqx} \ e^{i(2ia\gamma_L + \phi_L + qx)} ) \quad (\text{SM-25})$$

$$\langle \tilde{\psi} | x \in I_R \rangle = \frac{1}{\sqrt{2L}} ( e^{\gamma_R(a-L+x) - iqx} \ e^{\gamma_R(a+L-x) - 2iLq + iqx + i\phi_R} ) \quad (\text{SM-26})$$

### 2.3 – Retarded and advanced Green's functions

Using the previously obtained eigensystem of  $K$ , the retarded and advanced components of the Green's function for  $x, x' \in I_0$  are given by

$$\langle x | \mathbf{G}^R(\omega) | x' \rangle = \frac{1}{2L} \sum_n \begin{pmatrix} e^{i\phi_L} e^{-2a\gamma_L} e^{iq_n x} \\ e^{-iq_n x} \end{pmatrix} \frac{1}{\omega - vq_n} ( e^{-i\phi_L} e^{2a\gamma_L} e^{-iq_n x'} \ e^{iq_n x'} ) \quad (\text{SM-27})$$

and  $\mathbf{G}^A(\omega) = [\mathbf{G}^R(\omega)]^\dagger$ . The sum over the quantized  $q_n$ 's can be replaced by the contour integral

$$\frac{1}{2L} \sum_n \frac{e^{iq_n x}}{\omega - vq_n} = \oint_{z_i} \frac{dq}{2\pi} \frac{e^{iqx}}{\omega - vq} z_\pm(q) = \frac{i}{v} z_\pm(\omega v^{-1}) e^{i\omega v^{-1} x}, \quad (\text{SM-28})$$

where

$$z_\pm(q) = \frac{\pm 1}{e^{\pm[2iqL - 2a(\gamma_L + \gamma_R) + i(\phi_L - \phi_R)]} - 1}, \quad (\text{SM-29})$$



for  $x > 0$  or  $x < 0$  respectively, can be chosen in order to render the integral convergent once the contour is deformed. Using this identity we obtain

$$\begin{aligned} \langle x | \mathbf{G}^R(\omega) | x' \rangle = & i \frac{1}{v} \left[ \Theta(x - x') \begin{pmatrix} z_+(\omega v^{-1}) e^{i\omega v^{-1}(x-x')} & e^{i\phi_L} e^{-2a\gamma_L} z_+(\omega v^{-1}) e^{i\omega v^{-1}(x+x')} \\ e^{-i\phi_L} e^{2a\gamma_L} z_-(\omega v^{-1}) e^{-i\omega v^{-1}(x+x')} & z_-(\omega v^{-1}) e^{-i\omega v^{-1}(x-x')} \end{pmatrix} \right. \\ & \left. + \Theta(x' - x) \begin{pmatrix} z_-(\omega v^{-1}) e^{i\omega v^{-1}(x-x')} & e^{i\phi_L} e^{-2a\gamma_L} z_+(\omega v^{-1}) e^{i\omega v^{-1}(x+x')} \\ e^{-i\phi_L} e^{2a\gamma_L} z_-(\omega v^{-1}) e^{-i\omega v^{-1}(x+x')} & z_+(\omega v^{-1}) e^{-i\omega v^{-1}(x-x')} \end{pmatrix} \right] \end{aligned} \quad (\text{SM-30})$$

The spectral function is thus given by

$$\begin{aligned} \langle x | \boldsymbol{\rho}^-(\omega) | x' \rangle = & \frac{1}{2\pi v} \frac{\sinh(2a\gamma_L)}{\sinh[2a(\gamma_L + \gamma_R)]} \begin{pmatrix} e^{2a\gamma_R} u_{L,0}(\omega v^{-1}) e^{i\omega v^{-1}(x-x')} & e^{i\phi_L} u_{L,-2}(\omega v^{-1}) e^{i\omega v^{-1}(x+x')} \\ e^{-i\phi_L} u_{L,2}(\omega v^{-1}) e^{-i\omega v^{-1}(x+x')} & e^{-2a\gamma_R} u_{L,0}(\omega v^{-1}) e^{-i\omega v^{-1}(x-x')} \end{pmatrix} \\ & \frac{1}{2\pi v} \frac{\sinh(2a\gamma_R)}{\sinh[2a(\gamma_L + \gamma_R)]} \begin{pmatrix} e^{-2a\gamma_L} u_{L,0}(\omega v^{-1}) e^{i\omega v^{-1}(x-x')} & e^{i\phi_L} u_{L,0}(\omega v^{-1}) e^{i\omega v^{-1}(x+x')} \\ e^{-i\phi_L} u_{L,0}(\omega v^{-1}) e^{-i\omega v^{-1}(x+x')} & e^{2a\gamma_L} u_{L,0}(\omega v^{-1}) e^{-i\omega v^{-1}(x-x')} \end{pmatrix} \end{aligned} \quad (\text{SM-31})$$

where we defined

$$u_{L,n}(q) = -\frac{e^{i[qL + \frac{1}{2}(\phi_L - \phi_R)]n} \sinh[2a(\gamma_L + \gamma_R)]}{\cos[2qL + (\phi_L - \phi_R)] - \cosh[2a(\gamma_L + \gamma_R)]}. \quad (\text{SM-32})$$

In the limit  $L \rightarrow \infty$  one has that, for a regular function  $f(q)$  and  $\epsilon > 0$  independent of  $L$ ,

$$\lim_{L \rightarrow \infty} \frac{1}{2\epsilon} \int_{q-\epsilon}^{q+\epsilon} dq' u_{L,n}(q') f(q') = u_n f(q) \quad (\text{SM-33})$$

with

$$u_0 = 1 \quad (\text{SM-34})$$

$$u_{\pm 1} = 0 \quad (\text{SM-35})$$

$$u_{\pm 2} = e^{-2a(\gamma_L + \gamma_R)} \quad (\text{SM-36})$$

Using these limiting identities, for  $|x|, |x'| \ll L/2$  and  $L \rightarrow \infty$ , we can obtain the behavior of the spectral function, deep into the wire or closer to the boundaries:

$$\langle x | \boldsymbol{\rho}_{\text{bulk}}^-(\omega) | x' \rangle \equiv \langle x + L/2 | \boldsymbol{\rho}^-(\omega) | x' + L/2 \rangle = \frac{1}{2\pi v} \begin{pmatrix} e^{i\omega v^{-1}(x-x')} & 0 \\ 0 & e^{-i\omega v^{-1}(x-x')} \end{pmatrix} \quad (\text{SM-37})$$

$$\langle x | \boldsymbol{\rho}_{\text{left}}^-(\omega) | x' \rangle \equiv \langle x | \boldsymbol{\rho}^-(\omega) | x' \rangle = \frac{1}{2\pi v} \begin{pmatrix} e^{i\omega v^{-1}(x-x')} & e^{i\phi_L - 2a\gamma_L} e^{i\omega v^{-1}(x+x')} \\ e^{-i\phi_L - 2a\gamma_L} e^{-i\omega v^{-1}(x+x')} & e^{-i\omega v^{-1}(x-x')} \end{pmatrix} \quad (\text{SM-38})$$

$$\langle x | \boldsymbol{\rho}_{\text{right}}^-(\omega) | x' \rangle \equiv \langle x + L | \boldsymbol{\rho}^-(\omega) | x' + L \rangle = \frac{1}{2\pi v} \begin{pmatrix} e^{i\omega v^{-1}(x-x')} & e^{i\phi_R - 2a\gamma_R} e^{i\omega v^{-1}(x+x')} \\ e^{-i\phi_R - 2a\gamma_R} e^{-i\omega v^{-1}(x+x')} & e^{-i\omega v^{-1}(x-x')} \end{pmatrix} \quad (\text{SM-39})$$

## 2.4 – Keldysh Green's functions

In the steady state, the Keldysh component of the Green's function is given by  $G^K = G^R \Sigma^K G^A$  with  $\Sigma^K = \Sigma_L^K + \Sigma_R^K$  and

$$\langle x | \Sigma_l^K(\omega) | x' \rangle = -2iv\gamma_l \Theta(|x - x'| - a) \delta(x - x') \tanh\left[\frac{\beta_l}{2}(\omega - \mu_l)\right] \sigma_0, \quad (\text{SM-40})$$

this yields

$$\langle x | \mathbf{G}^K(\omega) | x' \rangle = \sum_{l=L,R} \int_{I_l} dy \langle x | \mathbf{G}^R(\omega) | y \rangle \langle y | \Sigma_l^K(\omega) | y \rangle \langle y | \mathbf{G}^A(\omega) | x' \rangle. \quad (\text{SM-41})$$

For  $x, x' \in I_0$  one gets

$$\begin{aligned} \langle x | \boldsymbol{\rho}^+ (\omega) | x' \rangle = & \tag{SM-42} \\ & \frac{1}{2\pi v} \tanh \left[ \frac{\beta_L}{2} (\omega - \mu_L) \right] \frac{\sinh (2a\gamma_L)}{\sinh [2a (\gamma_L + \gamma_R)]} \begin{pmatrix} e^{2a\gamma_R} u_{L,0} (\omega v^{-1}) e^{i\omega v^{-1}(x-x')} & u_{L,-2} (\omega v^{-1}) e^{i\phi_L} e^{i\omega v^{-1}(x+x')} \\ u_{L,2} (\omega v^{-1}) e^{-i\phi_L} e^{-i\omega v^{-1}(x+x')} & e^{-2a\gamma_R} u_{L,0} (\omega v^{-1}) e^{-i\omega v^{-1}(x-x')} \end{pmatrix} \\ & + \frac{1}{2\pi v} \tanh \left[ \frac{\beta_R}{2} (\omega - \mu_R) \right] \frac{\sinh (2a\gamma_R)}{\sinh [2a (\gamma_L + \gamma_R)]} \begin{pmatrix} u_{L,0} (\omega v^{-1}) e^{-2a\gamma_L} e^{i\omega v^{-1}(x-x')} & u_{L,0} (\omega v^{-1}) e^{i\phi_L} e^{i\omega v^{-1}(x+x')} \\ e^{-i\phi_L} u_{L,0} (\omega v^{-1}) e^{-i\omega v^{-1}(x+x')} & e^{2a\gamma_L} u_{L,0} (\omega v^{-1}) e^{-i\omega v^{-1}(x-x')} \end{pmatrix}. \end{aligned}$$

For  $|x|, |x'| \ll L/2$  and  $L \rightarrow \infty$ , we obtain

$$\begin{aligned} \langle x | \boldsymbol{\rho}_{\text{bulk}}^+ (\omega) | x' \rangle \equiv \langle x + L/2 | \boldsymbol{\rho}^+ (\omega) | x' + L/2 \rangle = & \\ & \frac{1}{2\pi v} \tanh \left[ \frac{\beta_L}{2} (\omega - \mu_L) \right] \frac{\sinh (2a\gamma_L)}{\sinh [2a (\gamma_L + \gamma_R)]} \begin{pmatrix} e^{2a\gamma_R} e^{i\omega v^{-1}(x-x')} & 0 \\ 0 & e^{-2a\gamma_R} e^{-i\omega v^{-1}(x-x')} \end{pmatrix} \\ & + \frac{1}{2\pi v} \tanh \left[ \frac{\beta_R}{2} (\omega - \mu_R) \right] \frac{\sinh (2a\gamma_R)}{\sinh [2a (\gamma_L + \gamma_R)]} \begin{pmatrix} e^{-2a\gamma_L} e^{i\omega v^{-1}(x-x')} & 0 \\ 0 & e^{2a\gamma_L} e^{-i\omega v^{-1}(x-x')} \end{pmatrix}; \end{aligned} \tag{SM-43}$$

$$\begin{aligned} \langle x | \boldsymbol{\rho}_{\text{left}}^+ (\omega) | x' \rangle \equiv \langle x | \boldsymbol{\rho}^+ (\omega) | x' \rangle = & \\ & \frac{1}{2\pi v} \tanh \left[ \frac{\beta_L}{2} (\omega - \mu_L) \right] \frac{\sinh (2a\gamma_L)}{\sinh [2a (\gamma_L + \gamma_R)]} \begin{pmatrix} e^{2a\gamma_R} e^{i\omega v^{-1}(x-x')} & e^{-2(a\gamma_L + a\gamma_R)} e^{i\phi_L} e^{i\omega v^{-1}(x+x')} \\ e^{-2(a\gamma_L + a\gamma_R)} e^{-i\phi_L} e^{-i\omega v^{-1}(x+x')} & e^{-2a\gamma_R} e^{-i\omega v^{-1}(x-x')} \end{pmatrix} \\ & + \frac{1}{2\pi v} \tanh \left[ \frac{\beta_R}{2} (\omega - \mu_R) \right] \frac{\sinh (2a\gamma_R)}{\sinh [2a (\gamma_L + \gamma_R)]} \begin{pmatrix} e^{-2a\gamma_L} e^{i\omega v^{-1}(x-x')} & e^{i\phi_L} e^{i\omega v^{-1}(x+x')} \\ e^{-i\phi_L} e^{-i\omega v^{-1}(x+x')} & e^{2a\gamma_L} e^{-i\omega v^{-1}(x-x')} \end{pmatrix}; \end{aligned} \tag{SM-44}$$

$$\begin{aligned} \langle x | \boldsymbol{\rho}_{\text{right}}^+ (\omega) | x' \rangle \equiv \langle x + L | \boldsymbol{\rho}^+ (\omega) | x' + L \rangle = & \\ & \frac{1}{2\pi v} \tanh \left[ \frac{\beta_L}{2} (\omega - \mu_L) \right] \frac{\sinh (2a\gamma_L)}{\sinh [2a (\gamma_L + \gamma_R)]} \begin{pmatrix} e^{2a\gamma_R} e^{i\omega v^{-1}(x-x')} & e^{i\phi_R} e^{i\omega v^{-1}(x+x')} \\ e^{-i\phi_R} e^{-i\omega v^{-1}(x+x')} & e^{-2a\gamma_R} e^{-i\omega v^{-1}(x-x')} \end{pmatrix} \\ & + \frac{1}{2\pi v} \tanh \left[ \frac{\beta_R}{2} (\omega - \mu_R) \right] \frac{\sinh (2a\gamma_R)}{\sinh [2a (\gamma_L + \gamma_R)]} \begin{pmatrix} e^{-2a\gamma_L} e^{i\omega v^{-1}(x-x')} & e^{-2(a\gamma_L + a\gamma_R)} e^{i\phi_R} e^{i\omega v^{-1}(x+x')} \\ e^{-2(a\gamma_L + a\gamma_R)} e^{-i\phi_R} e^{-i\omega v^{-1}(x+x')} & e^{2a\gamma_L} e^{-i\omega v^{-1}(x-x')} \end{pmatrix}; \end{aligned} \tag{SM-45}$$

## 2.5 – Bulk in the $L \rightarrow \infty$ limit

In the limit  $L \rightarrow \infty$ , the correlation functions within the bulk region becomes translational invariant  $\langle x | \boldsymbol{\rho}_{\text{bulk}}^\pm (\omega) | x' \rangle = \langle x - y | \boldsymbol{\rho}_{\text{bulk}}^\pm (\omega) | x' - y \rangle$ . One can thus consider the Fourier transformed quantities:

$$\boldsymbol{\rho}_{\text{bulk}}^\pm (\omega, q) = \int dx dx' e^{-iq(x-x')} \langle x | \boldsymbol{\rho}_{\text{bulk}}^\pm (\omega) | x' \rangle. \tag{SM-46}$$

Explicitly we obtain

$$\boldsymbol{\rho}_{\text{bulk}}^\pm (\omega, q) = \begin{pmatrix} \rho_L^\pm (\omega, q) & 0 \\ 0 & \rho_R^\pm (\omega, q) \end{pmatrix}, \tag{SM-47}$$

with

$$\begin{aligned} \rho_L^- (\omega, q) &= \delta (\omega - vq), \\ \rho_R^- (\omega, q) &= \delta (\omega + vq), \\ \rho_L^+ (\omega, q) &= F_L (\omega) \delta (\omega - vq), \\ \rho_R^+ (\omega, q) &= F_R (\omega) \delta (\omega + vq), \end{aligned}$$

where

$$F_L(\omega) = b_L \tanh \left[ \frac{\beta_L}{2} (\omega - \mu_L) \right] + (1 - b_L) \tanh \left[ \frac{\beta_R}{2} (\omega - \mu_R) \right] \quad (\text{SM-48})$$

$$F_R(\omega) = (1 - b_R) \tanh \left[ \frac{\beta_L}{2} (\omega - \mu_L) \right] + b_R \tanh \left[ \frac{\beta_R}{2} (\omega - \mu_R) \right] \quad (\text{SM-49})$$

and

$$e^{4a\gamma_L} = \frac{1 - b_R}{1 - b_L},$$

$$e^{4a\gamma_R} = \frac{b_L}{b_R}.$$

For the tight binding model, with  $r$  and  $r'$  in the middle of the wire, we obtain

$$\rho_{rr'}^\pm(\omega) \simeq a_0 \int_{-\Lambda}^{\Lambda} \frac{dq}{2\pi} \left[ \rho_L^\pm(\omega, q) e^{iq a_0(r-r')} e^{ik_F(r-r')} + \rho_R^\pm(\omega, q) e^{iq a_0(r-r')} e^{-ik_F(r-r')} \right], \quad (\text{SM-50})$$

or inverting the Fourier transform

$$\rho_k^\pm(\omega) = \rho_L^\pm[\omega, (k - k_F) a_0^{-1}] \Theta(|k - k_F| < \Lambda a_0) + \rho_R^\pm(\omega, k + k_F) \Theta(|k + k_F| < \Lambda a_0). \quad (\text{SM-51})$$

where  $k \in [0, 2\pi]$ .

The single particle density matrix, defined by

$$\varrho_{rr'}(t) = \langle c_r^\dagger(t) c_{r'}(t) \rangle, \quad (\text{SM-52})$$

that in the steady state is given by

$$\varrho_{rr'} = -\pi \int \frac{d\omega}{2\pi} \rho_{r'r}^+(\omega) + \frac{1}{2} \delta_{rr'},$$

can be approximated by

$$\varrho_{rr'} = \int_{-\pi}^{\pi} \frac{dk}{2\pi} e^{-i(r-r')k} n_k \quad (\text{SM-53})$$

with  $n_k$  the occupation number of the mode  $k$  given by

$$n_k \simeq \begin{cases} 1 & -k_F + a_0\Lambda < k < k_F - a_0\Lambda; \\ \frac{1}{2} \left\{ 1 - F_L \left[ \frac{v}{a_0} (k - k_F) \right] \right\} & \text{for } k_F - a_0\Lambda < k < k_F + a_0\Lambda; \\ 0 & k_F + a_0\Lambda < k \vee k < -k_F - a_0\Lambda; \\ \frac{1}{2} \left\{ 1 - F_R \left[ \frac{v}{a_0} (-k_F - k) \right] \right\} & \text{for } -k_F - a_0\Lambda < k < -k_F + a_0\Lambda; \end{cases}.$$

### 3 – IDENTIFICATIONS WITH THE TIGHT-BINDING MODEL II - $\phi_l$ AND $\gamma_l$

#### 3.1 – Self-energies

In the tight-binding model the self-energy contribution due to the reservoirs is given by

$$\Sigma_{\text{TB},rr'}^{R/A}(\omega) = \mp i \sum_l \Sigma_{\text{TB},rr';l}^{R/A}(\omega)$$

where

$$\Sigma_{\text{TB},rr';l}^{R/A}(\omega) = \mp i (\Gamma_l \delta_{r'r_l} \delta_{rr_l})$$

is the contribution from the reservoir  $l$  and  $\Gamma_l$  the hybridization constant [40]. The Keldysh component writes

$$\Sigma_{\text{TB},rr'}^K(\omega) = \sum_l \tanh \left[ \frac{\beta_l}{2} (\omega - \mu_l) \right] \left[ \Sigma_{\text{TB},rr';l}^R(\omega) - \Sigma_{\text{TB},rr';l}^A(\omega) \right].$$

### 3.2 – Determination of $\phi_l$

The tight-binding Hamiltonian, given by

$$\mathbf{H}_{\text{TB}} = -t \left[ \left( \sum_{r=0}^{N-2} |r\rangle \langle r+1| \right) + \text{h.c.} \right], \quad (\text{SM-1})$$

has wave functions of the form

$$\psi(r) = \langle r | \psi_k \rangle = A e^{ikr} + B e^{-ikr}, \quad (\text{SM-2})$$

and the dispersion relation

$$\varepsilon_k = -2 \cos(k). \quad (\text{SM-3})$$

Quantization condition for the momentum can be obtained imposing  $\langle r=0 | \mathbf{H}_{\text{TB}} | \psi_k \rangle = \varepsilon_k \langle 0 | \psi_k \rangle$  and  $\langle r=N-1 | \mathbf{H}_{\text{TB}} | \psi_k \rangle = \varepsilon_k \langle N-1 | \psi_k \rangle$  and are equivalent to the relations

$$\psi(-1) = \psi(N) = 0. \quad (\text{SM-4})$$

For the wave function expanded around  $k_{\text{F}}$

$$\langle r | \psi_k \rangle \simeq e^{ik_{\text{F}}r} \langle x = a_0 r | \psi_{\text{L}} \rangle + e^{-ik_{\text{F}}r} \langle x = a_0 r | \psi_{\text{R}} \rangle, \quad (\text{SM-5})$$

this implies, in the limit  $a_0 \rightarrow 0$ ,  $a_0 N \rightarrow L$ ,

$$e^{-ik_{\text{F}}} \langle 0 | \psi_{\text{L}} \rangle + e^{ik_{\text{F}}} \langle 0 | \psi_{\text{R}} \rangle = 0, \quad (\text{SM-6})$$

$$e^{ik_{\text{F}}La_0^{-1}} \langle L | \psi_{\text{L}} \rangle + e^{-ik_{\text{F}}La_0^{-1}} \langle L | \psi_{\text{R}} \rangle = 0, \quad (\text{SM-7})$$

yielding to the phase shifts

$$\phi_{\text{L}} = 2k_{\text{F}} - \pi, \quad (\text{SM-8})$$

$$\phi_{\text{R}} = -2k_{\text{F}}La_0^{-1} - \pi. \quad (\text{SM-9})$$

### 3.3 – Determination of $\gamma_l$

The eigensystem of

$$\mathbf{K}_{\text{TB}} = -t \left[ \left( \sum_{r=1}^{N-1} |r\rangle \langle r+1| \right) + \text{h.c.} \right] - i (\Gamma_{\text{L}} |1\rangle \langle 1| + \Gamma_{\text{R}} |N\rangle \langle N|),$$

that is the tight binding version of the  $\mathbf{K}$  operator, can be obtained in a similar way to the one of the previous section.

The spectrum of  $\mathbf{K}_{\text{TB}}$  is obtained imposing  $\langle r=0 | \mathbf{H}_{\text{TB}} | \psi_k \rangle = \varepsilon_k \langle 0 | \psi_k \rangle$  and  $\langle r=N-1 | \mathbf{H}_{\text{TB}} | \psi_k \rangle = \varepsilon_k \langle N-1 | \psi_k \rangle$ , and yields to

$$\left[ \frac{te^{-ik} - i\Gamma_{\text{L}}}{te^{ik} - i\Gamma_{\text{L}}} \right] \left[ \frac{te^{-ik} - i\Gamma_{\text{R}}}{te^{ik} - i\Gamma_{\text{R}}} \right] = e^{2ikN}.$$

Assuming  $k = k_0 + \frac{\Delta k}{N}$  where  $k_0$  is a solution of the equation

$$e^{-4ik_0} = e^{2ik_0N}, \quad (\text{SM-10})$$

i.e.

$$k_0 = \frac{\pi}{L+1} n \quad (\text{SM-11})$$

and  $\Delta k$  is of order  $1/N$ , we obtain

$$\Delta k = \frac{1}{2} \tan^{-1} \left\{ \frac{\sin(2k_0) [(\Gamma_R^2 + \Gamma_L^2) + 2 \cos(2k_0) \Gamma_L^2 \Gamma_R^2]}{\Gamma_L^2 \Gamma_R^2 \cos(4k_0) + (\Gamma_L^2 + \Gamma_R^2) \cos(2k_0) + t^2} \right\} + \frac{1}{4} i \left[ \ln \left( -\frac{\Gamma_L^2 t^{-2} - 2t^{-1} \sin k_0 \Gamma_L + 1}{\Gamma_L^2 t^{-2} + 2t^{-1} \sin k_0 \Gamma_L + 1} \right) + \ln \left( -\frac{\Gamma_R^2 t^{-2} - 2t^{-1} \sin k_0 \Gamma_R + 1}{\Gamma_R^2 t^{-2} + 2t^{-1} \sin k_0 \Gamma_R + 1} \right) \right]. \quad (\text{SM-12})$$

Therefore near  $k_0 = k_F$  we get

$$\text{Im} q = a_0^{-1} \text{Im}(k_0 - k_F) \quad (\text{SM-13})$$

$$= -\frac{1}{4} i \frac{1}{a_0 N} \left[ \ln \left( -\frac{\Gamma_L^2 t^{-2} + 2t^{-1} \sin k_F \Gamma_L + 1}{\Gamma_L^2 t^{-2} - 2t^{-1} \sin k_F \Gamma_L + 1} \right) + \ln \left( -\frac{\Gamma_R^2 t^{-2} + 2t^{-1} \sin k_F \Gamma_R + 1}{\Gamma_R^2 t^{-2} - 2t^{-1} \sin k_F \Gamma_R + 1} \right) \right]. \quad (\text{SM-14})$$

Identifying this expression with the quantization condition of the continuum model given by Eq.(SM-19) we obtain

$$a\gamma_l = \frac{1}{4} \ln \left( -\frac{\Gamma_l^2 t^{-2} - 2t^{-1} \sin k_F \Gamma_l + 1}{\Gamma_l^2 t^{-2} + 2t^{-1} \sin k_F \Gamma_l + 1} \right) \quad (\text{SM-15})$$

that for  $\Gamma_l \ll 1$  can be approximated by  $a\gamma_l \simeq \sin k_F \Gamma_l$ .

### 3.4 – Numerical results for the two-point function

Fig. 4 shows the one-point functions  $\rho_{rr'}^\pm(\omega)$  as a function of  $\omega$  for a finite system. The sharp features with frequency are signatures of the discrete spectrum of the finite chain in the absence of the leads and, in the spectral function  $\rho_{rr'}^-(\omega)$ , they become  $\delta$ -functions in the limit  $\Gamma_L, \Gamma_R \rightarrow 0$ . The infinite volume approximation washes out the rapid variations by averaging over small energy window of the order of the level spacing before taking the  $L \rightarrow \infty$  limit, see Eq.(SM-33).

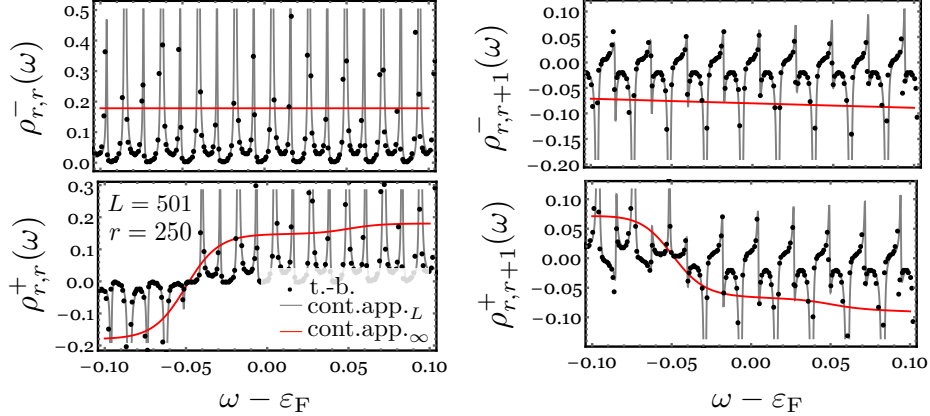


Figure 4. One-point functions  $\rho_{rr'}^\pm(\omega)$  as a function of  $\omega$  computed for  $r' = r$  (left panel) and  $r' = r + 1$  (right panel) and for  $r = 250$ ,  $L = 501$ ,  $\Gamma_L = 0.5t$ ,  $\Gamma_R = 0.2t$ ,  $\varepsilon_F = 0.9t$ ,  $V = 0.1t$ , and  $T_L = T_R = 0.01t$ . The black dots are obtained numerically using the tight-binding model. The black curves are obtained from the continuum limit for finite  $L$  using Eqs. (SM-31, SM-42). The infinite volume limit is obtained from Eqs.(SM-37-SM-39) and Eqs.(SM-43-SM-45).

## 4 – ENTANGLEMENT ENTROPY

### 4.1 – Derivation

The entanglement entropy of a region  $\Sigma$  is defined as

$$S_\Sigma = -\text{tr}(\hat{\rho}_\Sigma \ln \hat{\rho}_\Sigma) \quad (\text{SM-1})$$



where  $\hat{\rho}_\Sigma = \text{tr}_{\bar{\Sigma}} \hat{\rho}$  is obtained from the total density matrix  $\hat{\rho}$  by tracing out the degrees of freedom belonging  $\bar{\Sigma}$ , the complement of  $\Sigma$ . In the following we consider a region of size  $\ell$  in the central region of the wire

$$\Sigma_\ell = \{r : r \in [(L - \ell)/2, (L + \ell)/2]\}, \quad (\text{SM-2})$$

and we denote  $S_\ell = S_{\Sigma_\ell}$ . Since the model is Gaussian we have

$$S_\ell = \text{tr} [s(\varrho_\ell)] \quad (\text{SM-3})$$

for

$$s(\nu) = -\nu \ln \nu - (1 - \nu) \ln (1 - \nu) \quad (\text{SM-4})$$

with

$$\varrho_\ell = \sum_{rr' \in \Sigma_\ell} |r\rangle \varrho_{rr'} \langle r'| \quad (\text{SM-5})$$

We follow Ref. [41] and write

$$\begin{aligned} S_\ell &= \frac{1}{2\pi i} \oint dz s(\nu) \text{tr} \left[ \frac{1}{z - \varrho_\ell} \right] \\ &= \frac{1}{2\pi i} \oint dz s(\nu) \partial_z \ln \det [z - \varrho_\ell] \end{aligned} \quad (\text{SM-6})$$

The determinant can be calculated, asymptotically for  $\ell \rightarrow \infty$ , following Ref. [41] and using known results for approximating the determinant  $D_\ell[\phi] = \det [z - \varrho_\ell]$  of the Toplitz-like matrix  $z - \varrho_\ell$  with symbol

$$\phi(k) = z - n_k. \quad (\text{SM-7})$$

For the case  $T_R, T_L \neq 0$  the symbol  $\phi$  is smooth everywhere and thus the Szegö limit theorem yields to

$$D_\ell[\phi] \simeq E_{S_z}[\phi] e^{\ell \int \frac{d\theta}{2\pi} \ln \phi(\theta)}, \quad (\text{SM-8})$$

where  $E_{S_z}[\phi]$  is an  $\ell$  dependent constant, which gives

$$S_\ell = -\ell \sum_l \int_{-\infty}^{\infty} \frac{dk}{2\pi} s[n_k] + c^{\text{te}}. \quad (\text{SM-9})$$

For the case  $T_R, T_L = 0$  we have

$$n_k \simeq \begin{cases} 1 & -k_F + a_0\Lambda < k < k_F - a_0\Lambda \\ b_L & \text{for } k_F - a_0\Lambda < k < k_F + a_0\Lambda \\ 0 & k_F + a_0\Lambda < k \vee k < -k_F - a_0\Lambda \\ b_R & \text{for } -k_F - a_0\Lambda < k < -k_F + a_0\Lambda \end{cases}. \quad (\text{SM-10})$$

As the symbol  $\phi$  is not smooth and we have to use the Fisher-Hartwing conjecture[41] :

$$D_\ell[\phi] \simeq E_{\text{FH}}[\phi] e^{\ell V_0 + \ln(\ell) \sum_{j=0}^m (\alpha_j^2 - \beta_j^2)}, \quad (\text{SM-11})$$

with  $E_{\text{FH}}[\phi]$  an  $\ell$  independent constant where  $\beta_i$  and  $V(\theta)$  are defined by

$$\phi(\theta) = e^{V(\theta)} e^{i \sum_{i=0}^m \beta_i (\theta - \theta_i)} e^{-\pi \sum_{i=0}^m \beta_i \text{sgn}(\theta - \theta_i)} \left| 2 \sin \left( \frac{\theta - \theta_i}{2} \right) \right|^{2\alpha_j}, \quad (\text{SM-12})$$

and

$$V_0 = \int \frac{d\theta}{2\pi} V(\theta),$$

is the regular part. For our case we use the definitions

$$\theta_0 = 0; \theta_1 = k_F - \frac{\Delta}{2}; \theta_2 = k_F + \frac{\Delta}{2}; \theta_3 = 2\pi - k_F - \frac{\Delta}{2}; \theta_4 = 2\pi - k_F + \frac{\Delta}{2}; \quad (\text{SM-13})$$

and

$$\begin{aligned} \beta_0 &= 0; \\ \beta_1 &= \frac{1}{2\pi i} [\log(z-1) - \log(z-b_R)]; \beta_2 = \frac{i}{2\pi} [\log(z-b_R) - \log(z)]; \\ \beta_3 &= \frac{1}{2\pi i} [\log(z) - \log(z-b_L)]; \beta_4 = \frac{1}{2\pi i} [\log(z-b_L) - \log(z-1)]; \end{aligned} \quad (\text{SM-14})$$

and

$$e^{V(z)} = (z-1)^{\frac{2k_F - \Delta}{2\pi}} z^{\frac{-\Delta - 2k_F + 2\pi}{2\pi}} (z-b_L)^{\frac{\Delta}{2\pi}} (z-b_R)^{\frac{\Delta}{2\pi}}. \quad (\text{SM-15})$$

The entanglement entropy is therefore given by

$$S_\ell = \ell \left[ \frac{1}{2\pi i} \oint dz s(z) \partial_z V_0 \right] + \ln(\ell) \left[ \frac{1}{2\pi i} \oint dz s(z) \partial_z \sum_{j=0}^m (\alpha_j^2 - \beta_j^2) \right] \quad (\text{SM-16})$$

$$= \frac{\ell \Delta}{2\pi} [s(b_L) + s(b_R)] + \ln(\ell) \left[ \frac{1}{3} - \bar{s}(b_L) - \bar{s}(b_R) \right] + c^{\text{te}}, \quad (\text{SM-17})$$

where

$$\bar{s}(b) = \frac{1}{24} + \frac{1}{4\pi^2} [(2b-1) [\text{Li}_2(1-b) - \text{Li}_2(b)] + (1-b) \log^2(1-b) + b \log^2(b) + \log(b) \log(1-b)] \quad (\text{SM-18})$$

The contour of integration in Eq. (SM-16) contains the segment  $z \in [0, 1]$ .

## 4.2 – Additional numerical results

Fig.5 depicts the  $\ell$  and the  $\ln \ell$  coefficients of the entanglement entropy  $S_\ell$ , respectively  $\gamma_V$  and  $\tilde{\gamma}_V$ , as a function of the voltage. The numerical results obtained for the tight-binding model are seen to converge to the analytic curves predicted by the continuum model. We observe that  $\gamma_V \propto |V|$  and that  $\tilde{\gamma}_V$  is  $V$ -independent for  $V \neq 0$ . At  $V = 0$  we recover the equilibrium result  $\tilde{\gamma}_V = 1/3$ .

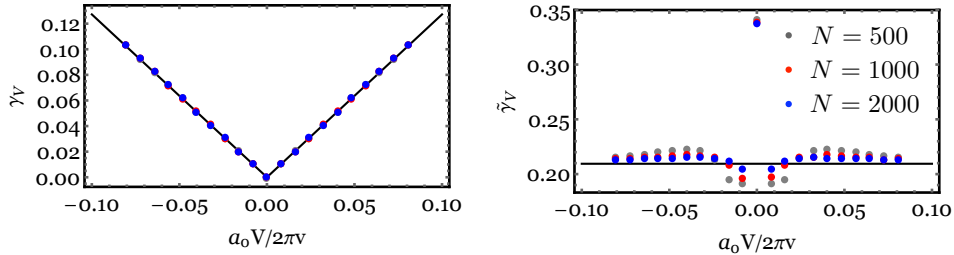


Figure 5. Volume,  $\gamma_V$ , and logarithmic,  $\tilde{\gamma}_V$ , coefficients of the entanglement entropy as a function of the applied voltage  $V$  computed for  $\Gamma_L = 0.02t$ ,  $\Gamma_R = 0.01t$ ,  $\varepsilon_F = 0.3t$ , and  $T_L = T_R = 0$ .

## 5 – TWO PARTICLE CORRELATION FUNCTIONS

The charge susceptibility, on the Keldysh contour  $\gamma$ , is defined as

$$\chi(zr, z'r') = -i \left[ \left\langle T_\gamma c_r^\dagger(z^+) c_r(z) c_{r'}^\dagger(z'^+) c_{r'}(z') \right\rangle - \left\langle T_\gamma c_r^\dagger(z^+) c_r(z) \right\rangle \left\langle T_\gamma c_{r'}^\dagger(z'^+) c_{r'}(z') \right\rangle \right], \quad (\text{SM-1})$$

where the  $z^+$  denotes a point coming infinitesimally later then  $z$  along  $\gamma$ . Due to the Gaussian nature of the model

$$\chi(zr, z'r') = -i G_{r'r'}(z', z) G_{r'r'}(z', z). \quad (\text{SM-2})$$

The greater and lesser components are given by  $\chi^{><}(\mathbf{tr}, t'\mathbf{r}') = \chi(z = \mathbf{tr}, z' = t'\mathbf{r}')$  with  $z$  respectively after or before  $z'$ . For the  $r$  and  $r'$  in the middle of the wire, using the approximated translational invariant Green's functions, we obtain:

$$\begin{aligned} \chi_{r,r'}^{><}(t, t') &= -i \left[ G_L^{<>}(t'x', tx) G_L^{><}(tx, t'x') + G_R^{<>}(t'x', tx) G_R^{><}(tx, t'x') \right] \\ &\quad -i \left[ G_L^{<>}(t'x', tx) G_R^{><}(tx, t'x') e^{-i2k_F(r-r')} + G_R^{<>}(t'x', tx) G_L^{><}(tx, t'x') e^{i2k_F(r-r')} \right] \end{aligned} \quad (\text{SM-3})$$

with  $x = ra_0$ ,  $x' = r'a_0$  and  $G_l(zx, z'x') = -i \langle T_\gamma \psi_l(zx) \psi_l^\dagger(z'x') \rangle$ , since the cross terms  $\langle T_\gamma \psi_R(zx) \psi_L^\dagger(z'x') \rangle$  vanish. Defining

$$G_l^a(tx, t'x') = \int \frac{d\omega}{2\pi} \int \frac{dq}{2\pi} e^{-i\omega(t-t')} e^{iq(x-x')} G_l^a(\omega k) \quad (\text{SM-4})$$

we have that, for the quantities  $\chi_p^\pm(\nu) = -\frac{1}{2\pi i} [\chi_p^>(\nu) \pm \chi_p^<(\nu)]$ ,

$$\chi_p^\pm(\nu) = [\chi_{LL}^\pm(\nu, a_0^{-1}p) + \chi_{RR}^\pm(\nu, a_0^{-1}p)] + \chi_{LR}^\pm[\nu, a_0^{-1}(p - 2k_F)] + \chi_{RL}^\pm[\nu, a_0^{-1}(p + 2k_F)] \quad (\text{SM-5})$$

with

$$\begin{aligned} \chi_{ll'}^\pm(\nu q) &= -\frac{1}{2\pi i} [\chi_{ll'}^>(\nu q) \pm \chi_{ll'}^<(\nu q)] \\ &= -\pi \int \frac{d\omega}{2\pi} \int \frac{dk}{2\pi} [\rho_l^\pm(\omega k) \rho_{l'}^\mp(\omega - \nu; k - q) - \rho_l^\mp(\omega k) \rho_{l'}^\pm(\omega - \nu; k - q)]. \end{aligned} \quad (\text{SM-6})$$

Explicitly, we obtain

$$\chi_{LL}^+(\nu q) = -\frac{1}{2v} \delta(\nu - vq) \int \frac{d\omega}{2\pi} [F_L(\omega) F_L(\omega - \nu) - 1], \quad (\text{SM-7})$$

$$\chi_{RR}^+(\nu q) = -\frac{1}{2v} \delta(\nu + vq) \int \frac{d\omega}{2\pi} [F_R(\omega) F_R(\omega - \nu) - 1], \quad (\text{SM-8})$$

$$\chi_{LR}^+(\nu q) = -\frac{1}{2v} \frac{1}{2\pi} \left[ F_L\left(\frac{vq + \nu}{2}\right) F_R\left(\frac{vq - \nu}{2}\right) - 1 \right], \quad (\text{SM-9})$$

$$\chi_{RL}^+(\nu q) = -\frac{1}{2v} \frac{1}{2\pi} \left[ F_R\left(\frac{-vq + \nu}{2}\right) F_L\left(\frac{-vq - \nu}{2}\right) - 1 \right], \quad (\text{SM-10})$$

and

$$\chi_{LL}^-(\nu q) = -\frac{1}{2v} \delta(\nu - vq) \int \frac{d\omega}{2\pi} [F_L(\omega - \nu) - F_L(\omega)], \quad (\text{SM-11})$$

$$\chi_{RR}^-(\nu q) = -\frac{1}{2v} \delta(\nu + vq) \int \frac{d\omega}{2\pi} [F_R(\omega - \nu) - F_R(\omega)], \quad (\text{SM-12})$$

$$\chi_{LR}^-(\nu q) = -\frac{1}{2v} \frac{1}{2\pi} \left[ F_R\left(\frac{vq - \nu}{2}\right) - F_L\left(\frac{vq + \nu}{2}\right) \right], \quad (\text{SM-13})$$

$$\chi_{RL}^-(\nu q) = -\frac{1}{2v} \frac{1}{2\pi} \left[ F_L\left(\frac{-vq - \nu}{2}\right) - F_R\left(\frac{-vq + \nu}{2}\right) \right]. \quad (\text{SM-14})$$